RSC Advances

ROYAL SOCIETY OF CHEMISTRY

www.rsc.org/advances

RSC Advances

PAPER

MWCNTs and nanoparticles composite as a high efficient and lightweight electromagnetic wave absorber in 4-18 GHz

Received 00th January 20xx,
Accepted 00th January 20xx

DOI: 10.1039/x0xx00000x

www.rsc.org/

Jiyong Fang, Yan Wang, Wei Wei, Zheng Chen, Yunxi Li, Zhi Liu, Xigui Yue* and Zhenhua Jiang

Nanoparticles decorated multi-wall carbon nanotubes nanocomposite (MWCNTs/Ag/$Co_{0.2}Fe_{2.8}O_4$) was designed and synthesized to meet the "wider, thinner, stronger" characteristics for an excellent electromagnetic (EM) wave absorber. The structure and morphology analyses demonstrated the structure of the nanocomposite absorber. The introduction of Ag nanoparticles can bring more interface and stronger coupling into the heterogeneous nanocomposite, while $Co_{0.2}Fe_{2.8}O_4$ can introduce dipoles and magnetic loss as well as more interfaces into the absorber. The electromagnetic parameters of absorber and wax composite with different absorber contents were measured at 2-18 GHz to evaluate its EM wave attenuation performance. With the absorber loading of 20%, at a thin thickness of 1.8 mm, the highest attenuation effectiveness value of -52.4 dB can be achieved at 10.2 GHz. Moreover, with the absorber thickness from 1.1 to 3.7 mm, the minimum RL value below -20 dB can be achieved at a wide range frequency from 4.0 to 18 GHz which covers the C band, the X band and the K_u band. Consequently, the nanocomposite absorber has an excellent EM wave attenuation ability with the characteristics of wide absorption band (4-18 GHz), strong absorption (-52.4 dB) and thin absorber thickness (1.1-3.7 mm). The excellent EM wave absorbency can be attributed to the strong interfacial and dipole polarization and Debye dipolar relaxation caused dielectric loss and the combination of the dielectric loss and the magnetic loss. It is believed that such a nanocomposite could serve as an attractive candidate for EM wave attenuation application in the future.

Introduction

In recent years, with the explosive development of the electronics industry and information technology, it is of profound importance to attenuate or shield the electromagnetic (EM) wave radiation around us which is not only threat to human health but also damage to other biological system. [1-4] Generally speaking, EM wave absorber is playing a critical role in providing solutions to EM wave radiation, and EM wave absorbers used in the microwave frequency range are in great demand for EM wave pollution prevention. [5] Hence, to solve this increasing deterioration of EM wave radiation problem, considerable efforts have already been taken in the fabrication of EM wave attenuation materials. As a consequence, various absorbers have been singled out or synthesized for EM wave attenuation, for instance, magnetic particles (Fe_3O_4, Co_3O_4, $CoFe_2O_4$, carbonyl iron, Fe_2O_3),[6-11] barium ferrite ($BaFe_{12}O_{19}$), [12] nanoparticles (Ag, Ni, Fe, Co, ZnO), [9, 13-16] conductive polymers (PANI, PPy), [17-19] carbon materials (CNTs, graphene, carbon powder, porous carbon), [20-24] and metallic perovskite lanthanum nickel oxide.[25] However, to the best of our knowledge, to be an excellent EM absorber, it should have wide absorption band width, strong EM wave absorption ability, thin matching thickness, tunable electromagnetic properties and high reliability, which can finally reward with a perfect EM wave attenuation. [16, 26] The thin thickness and low absorber loading can be beneficial to the fabrication of lightweight absorber and may make contribution to the application in military field. Nevertheless, it is arduous to achieve the above performance in a single absorber. Therefore, it is highly important to exploit new types of microwave absorption materials to meet the above "wider, thinner, stronger" characteristics for EM wave absorber.

In our previous work, a three-phase heterostructures absorber (CF/$Co_{0.2}Fe_{2.8}O_4$/PANI) with a layer by layer structure was specially designed and successfully synthesized in order to improve the EM wave absorbency of carbon fiber (CF). [27] CF/$Co_{0.2}Fe_{2.8}O_4$/PANI shows strong EM wave attenuation ability for the EM wave in the K_u band. The $Co_{0.2}Fe_{2.8}O_4$ nanoparticles are magnetic loss component which could not only optimize the EM parameters for a fine impedance matching, but also enhance the EM wave attenuation ability. However, CF has a relatively high density and the thermal stability of PANI is also unsatisfactory. Thus, the CF/$Co_{0.2}Fe_{2.8}O_4$/PANI absorber has fine EM wave attenuation performance with an absorber content of 40% which may be

The key laboratory for high performance polymer of the Ministry Education of China, College of Chemistry, Jilin University, 2699 Qianjin street, Changchun 130012, People's Republic of China. Email: yuexigui@jlu.edu.cn; Tel: +86-431-85168868

Electronic Supplementary Information (ESI) available: the selection of the absorber loading, EM wave attenuation performance of MWCNTs and MWCNTs/Ag, the dielectric loss tangent of all the materials and the Cole-Cole semicircles of all the samples. See DOI: 10.1039/x0xx00000x

an obstacle to application and it could not meet the great demand for high performance absorbers fine. Accordingly, to lower the absorber content and meet the "wider, thinner, stronger" characteristics, more scientific works are needed.

Multi-wall carbon nanotubes (MWCNTs), as an important member of the carbon material family, have been paid much attention as an EM wave attenuation material for its excellent mechanical properties, high electrical conductivity and ultra-light weight. [28] Thus, it can be a promising lightweight candidate for EM wave attenuation. [29, 30] However, according to the transmission line theory, it is hard to attain a desirable impedance matching condition for the unilateral dielectric loss materials. Thus the EM wave absorption ability is unsatisfying. To improve the EM wave attenuation performance of MWCNTs, several representative works have already been done. In the work of Qiu and et al, magnetite nanoparticle-carbon nanotube-hollow carbon fiber composites were prepared for EM wave absorption by chemical vapor deposition and chemical reaction.[31] The composites show strong absorbency for EM wave from 10.2 to 18 GHz (-50.9 dB at 14.03 GHz with 2.5 mm thickness), while for EM wave in 2-10 GHz, the absorbency is limited. Qing and et al reported that MWCNTs and carbonyl iron particles composites synthesized by a blending method show EM wave attenuation ability in 4-18 GHz with reflection loss (RL) lower than -10 dB.[28] However, the minimum reflection loss of the MWCNTs and carbonyl iron particles composites is just -16.9 dB. Besides, many other works have been done to further improve the EM wave attenuation ability. [17, 32-37] It is still hard to live up to the expectation for an excellent EM wave absorber with a wide absorption band, a strong absorbency intensity and a thin matching thickness.

In this work, for the improvement and continuation of our previous work, MWCNTs with the characteristics of excellent mechanical properties, high electrical conductivity and ultra-light weight, rather than CF, was selected as the lightweight candidate for EM wave attenuation to meet the expectation for an excellent EM wave absorber. To the best of our knowledge, magnetic particles are essential for EM wave absorbers in order to gain excellent EM wave absorbency, that is, a wide absorption band and a strong absorbency intensity. Because of the relatively fine EM wave absorption performance found in our previous work, $Co_{0.2}Fe_{2.8}O_4$ nanoparticles was sequentially used to enhance the EM wave absorption of MWCNTs. Nonmagnetic Ag nanoparticles with an attenuation mechanism different from PANI have the special surface effect, interface effect and quantum size effect which may enhance the EM wave absorbency. The Ag nanoparticles introduced on MWCNTs may enhance the interfacial polarizations between the Ag nanoparticles and other components due to the formation of a heterogeneous system and more interface, as well as the stronger coupling at the gaps between the adjacent Ag nanoparticles. Consequently, in this work, nanoparticles of Ag and $Co_{0.2}Fe_{2.8}O_4$ were specially selected and used to decorate MWCNTs. Accordingly, MWCNTs based absorber was designed. By introducing nanoparticles onto MWCNTs, the MWCNTs and nanoparticles composite absorber is expected to own an excellent EM wave attenuation ability. Also, the synergistic effect among the multiple components was expected to contribute to the finally EM wave performance of the nanocomposite absorber. The structure, morphology, complex permittivity and permeability, EM wave absorption and the attenuation mechanism of the absorber are investigated in detail.

Experimental

Materials

Multi-wall carbon nanotubes (MWCNTs, purity >99.9%, length ~50 μm) were supplied by Chengdu Organic Chemicals Co. Ltd and used as received. $FeCl_2 \cdot 4H_2O$ (Alfa Aesar), $CoCl_2 \cdot 6H_2O$ (Aladdin Chemistry Co. Ltd.) and $FeCl_3 \cdot 6H_2O$ (Sigma-Aldrich) were all used as received. $AgNO_3$, ammonium solution ($NH_3 \cdot H_2O$, 25%) and sodium citrate (Na_3Cit) were obtained from Sinopharm chemical Reagent Co. Ltd. and used without further purification.

Measurement

Fourier transform infrared (FT-IR) spectroscopy was performed on a Nicolet Impact 410 Fourier transform infrared (FT-IR) spectrometer and KBr was used as the nonabsorbent medium. A mixture of KBr and sample (weight ratio sample/KBr=1:100) was pressed into round-shaped sample. X-ray powder diffraction (XRD) was carried out using a PANalytical B.V. Empyrean system (Cu Kα) in the scattering range of 10°-80°. The magnetic properties of the synthesized materials were measured by a vibrating sample magnetometer (VSM) at 298 K (SQUID-VSM, America). Scanning electron microscopy (SEM) images were obtained on a FEI Nova Nano 450 field emission SEM system and samples were platinum coated. Transmission electron microscopic (TEM) images were obtained on a JEM-1200EX TEM system, coupled with the use of carbon-coated copper grids at a voltage of 100 kV. An Oxford X-Max energy dispersion X-ray spectrometry (EDS) system was applied to determine the elemental analysis information. The relative permeability and permittivity was obtained on an Agilent N5244A PNA-X network analyzer in the frequency range of 2–18 GHz for the calculation of reflection loss (RL) by the coaxial reflection/transmission method based on the NRW method. For microwave measurement, samples containing composite materials and paraffin wax with different weight ratios was pressed into toroidal-shaped samples (ϕ_{out}=7.00 mm, ϕ_{in}=3.04 mm).

Synthesis of the MWCNTs and nanoparticles composite (MWCNTs/Ag/$Co_{0.2}Fe_{2.8}O_4$)

The MWCNTs and nanoparticles composite was synthesized by a two-step reaction as shown in Fig. 1a. Firstly, 0.07 g $AgNO_3$ was added to a suspension of MWCNTs (A) in distilled water (400 ml, 1 mg/ml) and the mixture was heated to 100°C. Then 20 ml Na_3Cit solution (5 mg/ml) was dropwise added into the

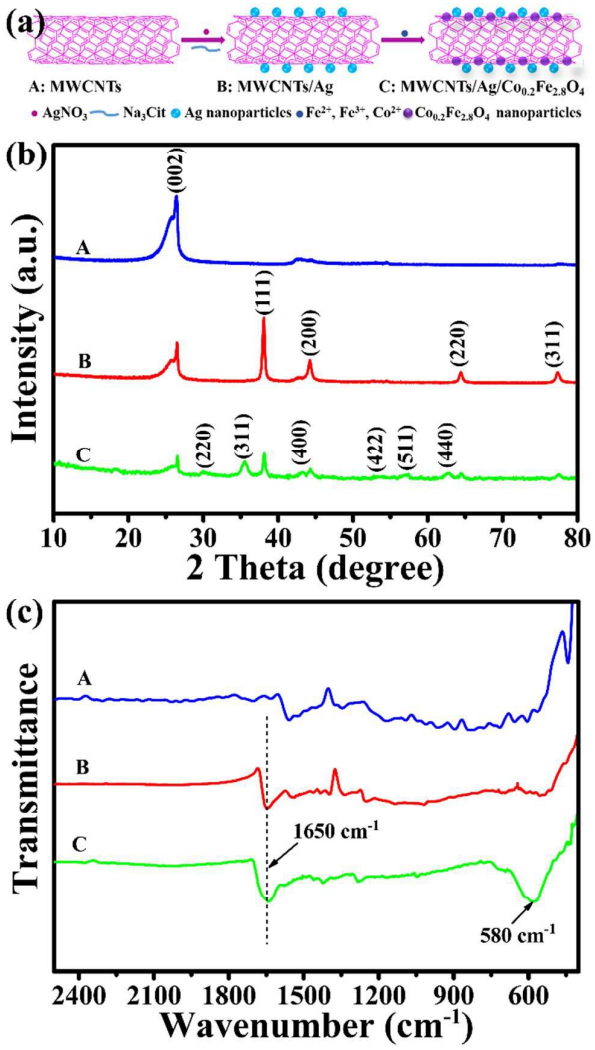

Fig.1. (a) The synthesis route of the MWCNTs and nanoparticles composite; (b) the XRD patterns of MWCNTs and the synthesized materials MWCNTs/Ag and MWCNTs/Ag/$Co_{0.2}Fe_{2.8}O_4$; (c) the FT-IR spectra of MWCNTs and the synthesized materials MWCNTs/Ag and MWCNTs/Ag/$Co_{0.2}Fe_{2.8}O_4$.

above mixture and kept at that temperature for 1 h for the completion of the reaction. After that, the product was filtered through a 0.45 μm millipore nylon filter membrane under vacuum, washed with distilled water and ethanol throughly, and dried in a vacuum oven for 12 h at 70°C. Thus, MWCNTs/Ag (B, 0.43 g) was obtained. Secondly, $FeCl_3 \cdot 6H_2O$ (2.1 mmol, 0.5676 g), $FeCl_2 \cdot 4H_2O$ (0.84 mmol, 0.1670g) and $CoCl_2 \cdot 6H_2O$ (0.21 mmol, 0.0500 g) were added to 400 ml suspension of the obtained MWCNTs/Ag (1 mg/ml, in water) with the protection of N_2. $Co_{0.2}Fe_{2.8}O_4$ magnetic nanoparticles were synthesized using a coprecipitation reaction. [38] The mixture was heated to 70°C. Then, $NH_3 \cdot H_2O$ was added to get a pH=10, and the mixture was kept at 70°C for 60 min. The obtained product was collected with the help of magnet field, followed by washing with water and ethanol for 5 times, respectively. The product was dried in a vacuum oven at 60°C for 12 h. Finally, MWCNTs and nanoparticles composite MWCNTs/Ag/$Co_{0.2}Fe_{2.8}O_4$ (C, 0.63 g) was obtained.

Results and Discussion

Structural and morphological analysis

In this work, Ag and $Co_{0.2}Fe_{2.8}O_4$ nanoparticles were used to decorate MWCNTs to achieve a better EM attenuation performance for the special surface effect, interface effect and quantum size effect caused EM wave attenuation of nanoparticles. MWCNTs were firstly decorated with the Ag nanoparticles by chemical reduction of $AgNO_3$. Then, magnetic $Co_{0.2}Fe_{2.8}O_4$ nanoparticles were precipitated on the surface of MWCNTs. To verify the structure of the synthesized nanocomposite, XRD and FT-IR were applied as shown in Fig. 1b and c.

The typical XRD patterns of sample A, B and C were shown in Fig. 1b. The obtained MWCNTs displays a relatively broad characteristic peak at 2θ=26.4°, indicating a hexagonal graphite with an index of (002) and a partially-crystalline nature of MWCNTs.[8] When MWCNTs was decorated with Ag, four more peaks were detected. Moreover, these four diffraction peaks are relatively sharp and strong, indicating that the Ag nanoparticles are highly crystalline. The obvious diffraction peaks at 2θ=37.9, 44.1, 64.4, and 77.3 can be assigned to the (111), (200), (220), and (311) planes of face-centered-cubic structure of Ag, respectively,[39] indicating that the crystallized Ag nanoparticles could be obtained by Na_3Cit chemical reduction.[40]

When MWCNTs were further coated with $Co_{0.2}Fe_{2.8}O_4$, for sample C, six more diffraction peaks were observed which are belong to $Co_{0.2}Fe_{2.8}O_4$. However, the peaks are relatively broad, suggesting the small size of the magnetic particles. The series of diffraction peaks at 2θ = 30.2°, 35.5°, 43.2°, 53.6°, 57.3°and 63.0°are assigned to the (220), (311), (400), (422), (511) and (440) planes of the face centered cubic lattice of $Co_{0.2}Fe_{2.8}O_4$, respectively. [15] The absence of impurity peaks in the XRD pattern indicates that the synthesized $Co_{0.2}Fe_{2.8}O_4$ nanoparticles have a high degree of purity.

Fig. 1c shows the FT-IR spectra of MWCNTs (A), MWCNTs/Ag (B), and MWCNTs/Ag/$Co_{0.2}Fe_{2.8}O_4$ (C). In the FT-IR spectrum of sample B, there is a relatively strong absorption peak at 1650 cm^{-1} compared to that of sample A. The new peak in sample B belongs to the stretching vibration of the carbonyl groups of Na_3Cit which is absorbed on the surface of the Ag nanoparticles. As MWCNTs/Ag was synthesized with $AgNO_3$ and Na_3Cit, the new peak can also be an evidence of the Ag nanoparticles in the composite. In contrast to the spectra of sample A and B, strong absorption peak at 580 cm^{-1} (Fe-O stretching vibration) appears in that of C, which demonstrates the existence of the $Co_{0.2}Fe_{2.8}O_4$ nanoparticles in the nanocomposite.

Moreover, EDS technique was further used to verify the structure of the synthesized materials. As shown in Fig. 3a, for MWCNTs/Ag, elements of Ag and C were detected. Hence, the EDS data can be an evidence for the successful synthesis of Ag

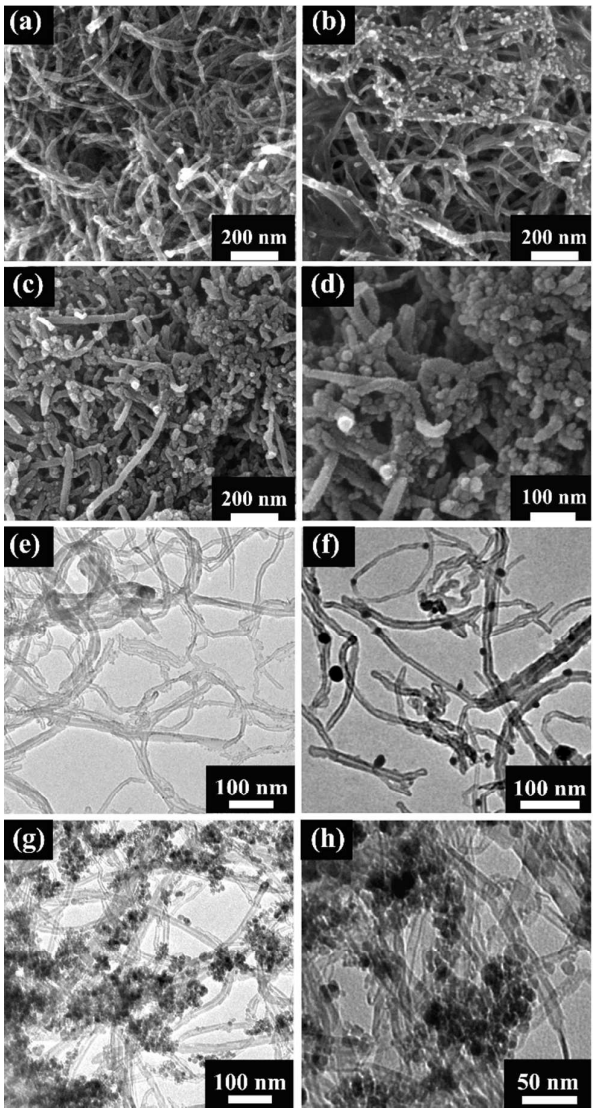

Fig. 2. (a) SEM image of the as-received MWCNTs; (b) SEM image of MWCNTs/Ag; (c and d) SEM images of MWCNTs/Ag/$Co_{0.2}Fe_{2.8}O_4$ with different scale; (e) TEM image of the as-received MWCNTs; (f) TEM image of MWCNTs/Ag; (g and h) TEM images of MWCNTs/Ag/$Co_{0.2}Fe_{2.8}O_4$ with different scale.

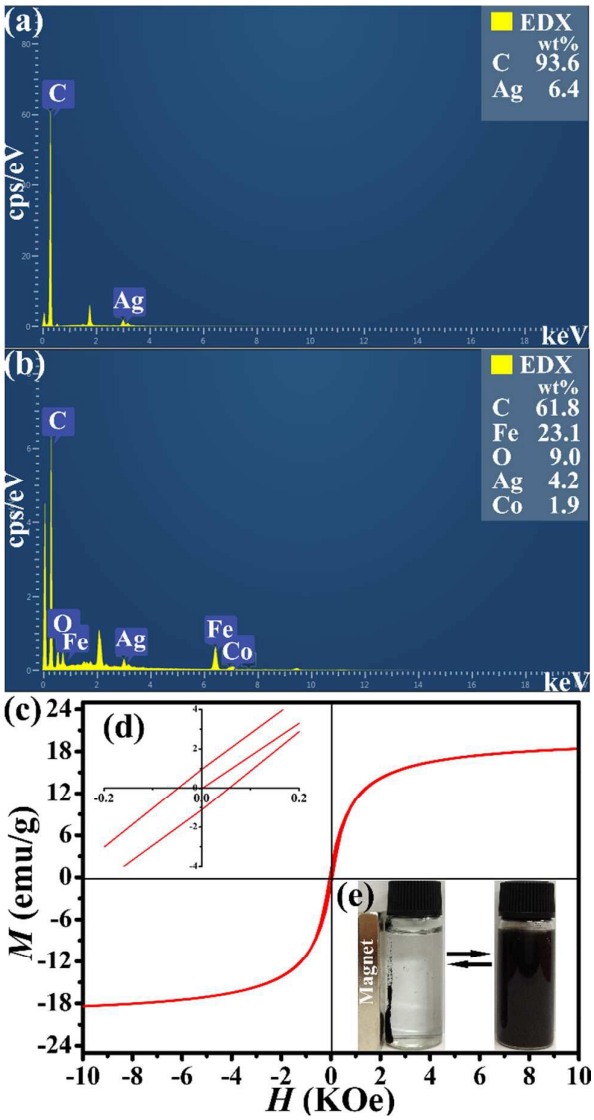

Fig. 3. (a) the EDS elemental data of MWCNTs/Ag; (b) the EDS elemental data of MWCNTs/Ag/$Co_{0.2}Fe_{2.8}O_4$; (c) *M-H* loops of MWCNTs/Ag/$Co_{0.2}Fe_{2.8}O_4$; (d) *M-H* loops of MWCNTs/Ag/$Co_{0.2}Fe_{2.8}O_4$ in a low field region; (e) photo of MWCNTs/Ag/$Co_{0.2}Fe_{2.8}O_4$ with and without magnet filed.

nanoparticles by Na_3Cit reduction. Fig. 3b shows the obtained EDS data of the as synthesized MWCNTs/Ag/$Co_{0.2}Fe_{2.8}O_4$ absorber. Thus, for MWCNTs/Ag/$Co_{0.2}Fe_{2.8}O_4$, after coating with $Co_{0.2}Fe_{2.8}O_4$, elements of Fe, Co, and O were observed which can be evidence of the $Co_{0.2}Fe_{2.8}O_4$ in the nanocomposite. Hence, according to the above XRD, IR and EDS results, MWCNTs and nanoparticles composite was successfully synthesized as expected.

To the best of our knowledge, the dispersed situation of the nanoparticles in MWCNTs will have great influence on the characteristics of the synthesized material. Here, to investigate the dispersion situation of the nanoparticles in MWCNTs, SEM and TEM techniques were taken as stretched in Fig. 2. Compared to the SEM image of MWCNTs in Fig. 2a, for MWCNTs/Ag shown in Fig. 2b, there are many nanoparticles on the surface of MWCNTs which are the Na_3Cit reduced Ag nanoparticles. The nanoparticles are relatively well dispersed on the surface of MWCNTs, indicating the strong interaction between Ag nanoparticles and MWCNTs. The nanoparticles have an average diameter of 20 nm. When MWCNTs was further coated with $Co_{0.2}Fe_{2.8}O_4$ as shown in Fig. 2c and 2d, obviously, the surface of MWCNTs became rough and magnetic nanoparticles $Co_{0.2}Fe_{2.8}O_4$ were randomly coated on the surface of MWCNTs. Also, the TEM images can be a strong evidence. As shown in Fig. 2f, after the reduction of $AgNO_3$ by Na_3Cit, several nanoparticles appeared on the surface of the MWCNTs when compared to the TEM images of MWCNTs (Fig. 2e). The Ag nanoparticles on the wall of MWCNTs have a diameter of 18 nm on average. The diameter of the Ag

nanoparticles determined by TEM happens to coincide with the result of SEM. When MWCNTs were further decorated with $Co_{0.2}Fe_{2.8}O_4$, more nanoparticles with a diameter of 10 nm appeared. As stretched in Fig. 2g and 2h, the $Co_{0.2}Fe_{2.8}O_4$ magnetic particles distribute randomly on the wall of MWCNTs. Therefore, according to the above results (XRD, FT-IR, EDS, SEM and TEM), the MWCNTs and nanoparticles composite was synthesized as expected. And the successful synthesis of nanocomposite absorber will endow it with some exceptional properties, for instance, magnetic property, permittivity and permeability.

Magnetic property

In this specially designed nanocomposite absorber, $Co_{0.2}Fe_{2.8}O_4$ nanoparticles performed as a promoter to increase the complex permeability of the microwave absorber to achieve a fine matching condition. The specially designed magnetic $Co_{0.2}Fe_{2.8}O_4$ nanoparticles was synthesized in our previous work and selected for EM wave attenuation application. [38] In this work, it was continued to be used to bring the composite absorber with magnetic loss ability. Undoubtedly, the magnetic property of the synthesized absorber is important. The magnetic property of the synthesized absorber was investigated at room temperature by measuring its magnetization curves. The magnetization hysteresis loop (*M-H*) of MWCNTs/Ag/$Co_{0.2}Fe_{2.8}O_4$ (Fig. 3c and 3d) demonstrates the nanocomposite maintain good superparamagnetic property of the $Co_{0.2}Fe_{2.8}O_4$ nanoparticles with the M_s reached to 18.4 emu/g. The nonmagnetic components of carbon and Ag in the absorber reduce the effective mass/volume percentage of $Co_{0.2}Fe_{2.8}O_4$, thus relatively less hysteresis was observed. Moreover, when a magnet is placed beside a bottle filled with a suspension of MWCNTs/Ag/$Co_{0.2}Fe_{2.8}O_4$ in water, the composite MWCNTs/Ag/$Co_{0.2}Fe_{2.8}O_4$ quickly move along the magnetic field and completely deposit near the magnet and the solution becomes colorless, as shown in Fig. 3e. Thus, MWCNTs/Ag/$Co_{0.2}Fe_{2.8}O_4$ has a strong response to magnetic field. To conclude, for MWCNTs/Ag/$Co_{0.2}Fe_{2.8}O_4$, the saturation magnetization produced by $Co_{0.2}Fe_{2.8}O_4$ nanoparticles may improve the low-frequency complex permeability, as shown in Fig. 5. The improved magnetic property is favorable for natural resonance loss and eddy current loss, leading to enhanced magnetic loss. Additionally, it is believable the magnetic property may contribute to the complex permeability to achieve a relatively fine matching condition between the complex permittivity and permeability.

Permittivity and permeability

It is well known that the microwave absorbency of an absorber highly depend on its electromagnetic parameters, i.e., the complex permittivity (ε_r) and complex permeability (μ_r), where the real parts of permittivity and permeability represent the storage capability of EM wave energy, and the imaginary parts of permittivity and permeability represent the loss capability of EM wave energy. Hence, to confirm the relative complex permittivity and permeability, the paraffin wax based MWCNTs/Ag/$Co_{0.2}Fe_{2.8}O_4$ composites were fabricated with different absorber weight contents. To be lightweight, the loading of the absorber should be as low as possible and the lower the better. In this work, the absorber content was investigated form 5% to 20%. The complex permittivity ($\varepsilon_r=\varepsilon'-j\varepsilon''$) (Fig. 4) and complex permeability ($\mu_r=\mu'-j\mu''$) (Fig. 5) were observed in the EM wave frequency range 2−18 GHz.

With the increase of absorber content, as shown in Fig. 4, both the real part (ε′) and imaginary part (ε″) of permittivity are obviously enhanced and become more and more dependent on the EM wave frequency especially with a higher absorber content. With a higher loading of absorber, the content of high electrical conductivity MWCNTs increases, which is favorable for high complex permittivity according to the free electron theory. [41] Moreover, to the best of our knowledge, some pristine carbon materials, for instance, graphene, carbon nanotubes, and carbon fibers, commonly display a frequency dispersion behavior in the EM wave frequency range of 2−18 GHz, that is, their complex permittivity will gradually decrease with the increasing frequency. [41] Also this dispersion behavior still exist in most carbon materials and magnetic materials

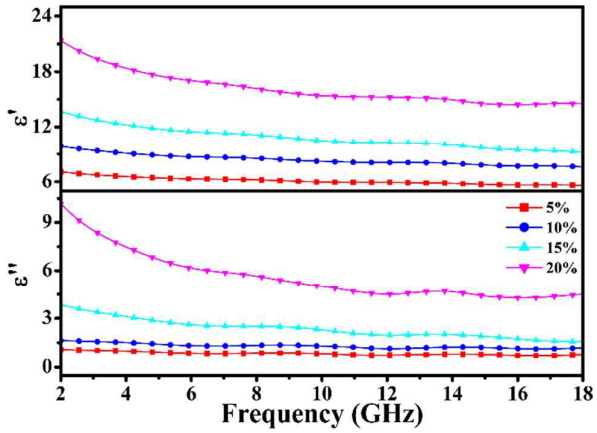

Fig. 4. The relative permittivity of MWCNTs/Ag/$Co_{0.2}Fe_{2.8}O_4$ with absorber content of 5%, 10%, 15%, and 20%. The real part and the imaginary part of permittivity have the same curve label.

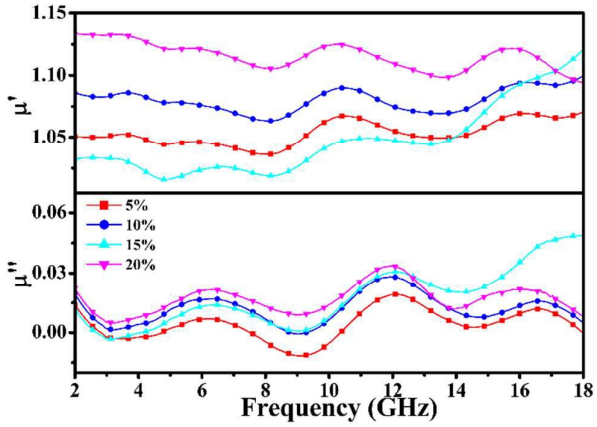

Fig. 5. The relative permeability of MWCNTs/Ag/$Co_{0.2}Fe_{2.8}O_4$ with absorber content of 5%, 10%, 15%, and 20%. The real part and the imaginary part of permeability have the same curve label.

composites. Here, in this work, a similar distinguishable frequency dispersion behavior is also observed. With the absorber content higher than 10%, both ε' and ε" decrease rapidly with frequency. However, the ε' values are all higher than 6, while ε" values are all higher than 1.2. And the relatively high ε" values indicate a strong dielectric loss ability of the nanocomposite absorber. It was suggested that the nanocomposite had obvious dielectric loss properties, better energy storage and dissipation capability.

For permeability, as displayed in Fig. 5, with the increase of absorber content, the real part (μ') and the imaginary part (μ") of permeability were enhanced with exceptions at an absorber content of 15% for μ'. Similar exceptions are also observed in other magnetic materials. [42] Additionally, there is a normal resonance phenomenon between μ' and μ" with the increasing of EM wave frequency. These high resonance frequencies are mainly attributed to the small size effect and confinement effect. [38] Because the rotation of domains in magnetic nanocrystals became difficult due to the effective anisotropy, the induced magnetization lags behind the applied field resulted in magnetic losses when the magnetic dipole tried to rotate with the frequency. It was considered the effective anisotropy energy could be remarkably enhanced with decreasing nanoparticles size, due to the surface anisotropic field and microstructure defects. [38] To conclude, the special permittivity and permeability together will contribute to the final EM wave attenuation performance.

Microwave absorption properties

When EM wave is incident on the surface of the absorber, part of the wave energy is reflected on the surface and the wave inside the absorber is attenuated. The reflection on the surface is determined by the input characteristic impedance (Z_{in}) and the characteristic impedance of free space (Z_0): [43]

$$\Gamma=(Z_{in}-Z_0)/(Z_{in}+Z_0) \quad (1)$$

Moreover, the EM wave attenuation ability inside the absorber is related to the attenuation constant α expressed as: [44]

$$\alpha=\frac{\pi f}{c}\sqrt{2\mu'\varepsilon'}\sqrt{\frac{\mu''\varepsilon''}{\mu'\varepsilon'}-1+\sqrt{\left(\frac{\mu''}{\mu'}\right)^2+\left(\frac{\varepsilon''}{\varepsilon'}\right)^2+\left(\frac{\mu''\varepsilon''}{\mu'\varepsilon'}\right)^2+1}} \quad (2)$$

Undoubtedly, as mentioned above, both the reflection factor (Γ) and the attenuation constant (α) are function of the electromagnetic parameters of the absorber. Furthermore, it is well known that the real parts and the imaginary parts of the relative complex permittivity and the relative complex permeability represent the storage and loss of EM wave energy, respectively. Accordingly, the EM wave absorbency of absorber can be determined by the obtained electromagnetic parameters of the synthesized absorber. [27] Based on the above measured EM parameters shown in Fig. 4 and 5, i.e., the complex permittivity and permeability, the simulated EM wave reflection loss (RL, in dB unit) of MWCNTs/Ag/$Co_{0.2}Fe_{2.8}O_4$ with different absorber loadings was investigated based on the transmission line theory evaluated by the following equations:

$$RL=20\lg\left|(Z_{in}-Z_0)/(Z_{in}+Z_0)\right| \quad (3)$$

$$Z_0=\sqrt{\mu_0/\varepsilon_0} \quad (4)$$

$$Z_{in}=Z_0\sqrt{\mu_r/\varepsilon_r}\tanh[j(2\pi fd/c)\sqrt{\mu_r\varepsilon_r}] \quad (5)$$

where Z_0 is the characteristic impedance of free space (air), μ_0 and ε_0 are the complex relative permeability and permittivity of free space (air), while Z_{in} is the input characteristic impedance, f is the EM wave frequency in Hz unit, d is the thickness of the absorber material, c is the velocity of electromagnetic waves in free space which equals to 3×10^8 m/s. and ε_r and μ_r are the complex permittivity ($\varepsilon_r=\varepsilon'-j\varepsilon''$) and permeability ($\mu_r=\mu'-j\mu''$) of the absorber, respectively. [41, 45]

It is well known that the absorber loadings are important to the final EM wave attenuation ability. To be lightweight, the absorber content should not be high. In this work, the simulated reflection loss-frequency (RL-F) curves with different absorber contents (5%, 10%, 15%, and 20%) are illustrated in the supporting information (See section SI-1, Figure S1, S2, S3 and S4). The RL values vary with the mass content of the MWCNTs/Ag/$Co_{0.2}Fe_{2.8}O_4$ absorber in wax matrix. It is found that with the absorber content of 20%, the nanocomposite absorber shows the greater EM absorbing properties and has the potential to meet the strict requirements (wider, thinner and stronger) for EM wave absorber.

To further verify the EM wave attenuation ability of the nanocomposite at 20% loading, the RL-F curves were refined with the absorber thickness from 1.1 to 3.7 mm, and it is found to be sensitive to the absorber sample thickness. With increasing in the absorber sample thickness, the strong peak positions all have a tendency toward lower frequency range. According to the quarter-wavelength cancellation model, it is known that the minimal reflections can be achieved at a certain EM wave frequency if the thickness of the absorber composite satisfies the following matching equation.[46]

$$d=nc/(4f\sqrt{|\varepsilon_r||\mu_r|}) \quad (n=1, 3, 5\ldots) \quad (6)$$

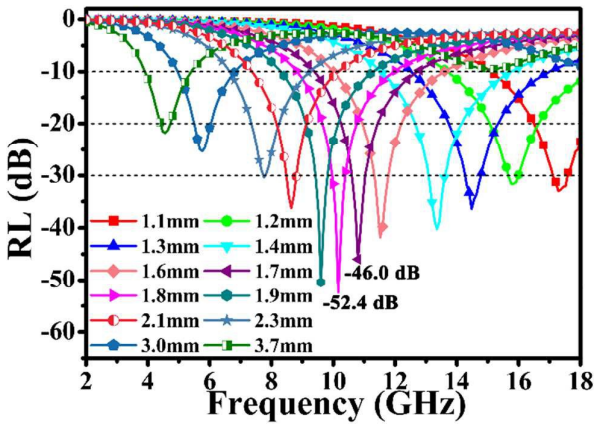

Fig. 6. The relationship between RL-F for MWCNTs/Ag/$Co_{0.2}Fe_{2.8}O_4$ at absorber content of 20% with absorber thickness from 1.1 to 3.7mm.

Consequently, the attenuation peaks shift to the lower frequency regions and more attenuation peaks might appear as the thickness of the absorbers increases. As shown in Fig. 6, with absorber thickness from 1.1 to 3.7 mm, the absorber shows a strong absorbency for EM wave in the C band, the X band and the K_u band with RL values below -10 dB (90% attenuation). In the C band, at a thickness of about 2.3 mm, the strongest absorption could be achieved at 7.8 GHz with RL value of -30.4 dB. And with the absorber thickness from 2.3 to 3.7 mm, the minimum RL values are below -20 dB, which indicates that more than 99% of the EM wave can be attenuated at this region. In the X band, when the absorber thickness was 1.8 mm, the strongest RL of -52.4 dB was observed at 10.2 GHz (more than 99.999% attenuation). With the absorber thickness of 1.6-2.1 mm, the minimum RL values are all below -35 dB, indicating a strong attenuation ability of this nanocomposite absorber in the EM wave X band. In the K_u band, at a thickness of 1.2 mm, a minimum RL of -31.6 dB was obtained at 15.8 GHz and the RL below -10 dB could be achieved from 13.7 to 18 GHz. Moreover, with the increasing in absorber thickness (1.1 to 1.4 mm), the EM wave absorbency was enhanced and the minimum RL values are all below -30 dB. Accordingly, at this absorber content (20%), the nanocomposite absorber has excellent EM wave attenuation ability with the wide absorption band (4-18 GHz), the strong absorption (minimum RL value of -52.4 dB at 10.2 GHz) and the thin absorber thickness (RL value of -52.4 dB at 1.8 mm, and the strong absorption in 4-18 GHz with thickness of 1.1-3.7 mm). Additionally, the strong absorption can benefit the efficiency of the absorber, while the low absorber loading (20%) and the thin absorber thickness can contribute to the fabrication of lightweight EM wave-absorbing materials. Comparison with other MWCNTs based absorbers listed in Table 1, MWCNT/Ag/$Co_{0.2}Fe_{2.8}O_4$ synthesized in this work has great advantages considering the absorber loading, the absorbency, the absorber thickness and the absorption frequency width. This suggests that the nanocomposite absorber synthesized in this work can be an attractive candidate for EM wave absorber.

Table 1 The EM wave absorption performance of the MWCNTs based absorbers

Absorber	Loading (%)	RL_{min} (dB)	Thickness[a] (mm)	FR[b] (GHz)
MWCNT-Fe[33]	10	-29.4	3.4	7.4-18
Fe_3O_4-CNTs-HPCFs [31]	20	-50.9	2.5	9.0-18
CNT@Fe@SiO_2 [47]	50	-22.0	3.0	5.5-18
MWCNTs/Fe [37]	60	-39.0	4.3	2.0-3.5[c]
BTO/CNT [48]	60	-56.5	1.1	9.6-14
$BaTiO_3$/MWNT/PBO [36]	80	-45.5	3.0	6.5-16
MWCNT/Ag/$Co_{0.2}Fe_{2.8}O_4$ (this work)	20	-52.4	1.8	4.0-18

[a] the absorber thickness corresponding to the minimum RL value

[b] FR: the frequency range with RL<-10 dB achieving by the variation of the absorber thickness

[c] the frequency range with the RL<-20 dB achieving by the variation of the absorber thickness

For comparison and to express the importance of this specially designed structure, the simulated reflection loss-frequency (RL-F) curves of MWCNTs and MWCNTs/Ag are presented in the supporting information (See section SI-2 and SI-3). As shown in Figure S5, the EM wave absorbency of MWCNTs with the loading of 12.4% (20%×61.8%=12.4%) is not satisfactory. The minimum RL values are all higher than -12 dB in the EM wave frequency of 2-18 GHz. However, for MWCNTs/Ag, as sketched in Figure S6, the EM wave absorption ability has been improved especially in the low frequency region. In the C band, a minimum RL value of -35.6 dB is obtained at 4.3 GHz with the absorber thickness of 5.5 mm. Undoubtedly, the EM wave absorbency is improved by the modification of MWCNTs with Ag nanoparticles. Moreover, as shown in Fig. 6, with the further decoration of the $Co_{0.2}Fe_{2.8}O_4$ magnetic nanoparticles, the EM wave attenuation ability is enhanced with the wide absorption width, the thin matching thickness and the strong absorbency. Accordingly, the specially designed nanostructure has great influence on the final EM wave attenuation performance of the nanocomposite absorber.

As is well known, when the incident EM wave is interacted with the absorber, part of the EM wave is reflected on the surface of the absorber, while part of the EM wave is attenuated inside the absorber and then transmitted as shown in Fig. 7a. An excellent absorber can reduce the reflection and increase the absorption at the greatest degree. To be an excellent absorber, there are two key factors that should be taken into consideration. One is the impedance matching condition, which allows EM wave to propagate into the absorber sufficiently and avoids the strong reflection, this is also the precondition of EM wave absorption. [49] It is well known that in an optimal situation, the EM matching is illustrated by the equation: $\mu''=\varepsilon''$ and $\mu'=\varepsilon'$. However, the permittivity and permeability can't meet the above equation in different frequencies in the same medium because both of permittivity and permeability are function of frequency. Also, for most synthesized composite materials, the permittivity is usually higher than permeability. In this work, $Co_{0.2}Fe_{2.8}O_4$ nanoparticles with relatively low conductivity was used to decorate MWCNTs. Apparently, the higher impedance values would lead to lower reflection effectiveness, though an optimal matching condition is not achieved. [24] Thus, as shown in Fig. 7a, EM wave can propagate into the absorber to be attenuated rather than reflected on the absorber surface. Hence, the $Co_{0.2}Fe_{2.8}O_4$ nanoparticles play an important role in determining the EM wave absorption characteristic of this MWCNTs based nanocomposite absorber. The other key factor is the best EM wave attenuation performance inside the absorber. An excellent absorber can attenuate the incident EM wave rapidly through the absorber layer, and reduce the emerging wave to an acceptable low magnitude. [49] It is well known that when an EM wave is incident on the absorber sample, there are two possible contributions for the EM wave absorption, that is, the dielectric loss and the magnetic loss. [50] In addition, a higher value of loss tangent indicates a higher EM wave loss. Fig. 7c shows the calculated dielectric loss

tangent ($\tan\delta_\varepsilon=\varepsilon''/\varepsilon'$) and magnetic loss tangent ($\tan\delta_\mu=\mu''/\mu'$) of the synthesized nanocomposite with different absorber content. In the EM wave frequency range 2-18 GHz, for all absorber content, the dielectric loss tangent is higher than the magnetic loss tangent, suggesting a better dielectric loss ability than magnetic loss ability for this nanocomposite absorber. [17] At the absorber loading of 20%, the composite shows the strongest dielectric loss and magnetic loss ability. Thus, at this content, EM wave energy can be effectively converted into heat or other forms absorbed by materials and the EM wave is thus attenuated inside the absorber as demonstrated in Fig. 7a. [51] Moreover, for comparison, the dielectric loss tangent of MWCNTs and MWCNTs/Ag are presented in the supporting information (section SI-4, Figure S7). With the decoration of MWCNTs by the Ag nanoparticles and the $Co_{0.2}Fe_{2.8}O_4$ magnetic nanoparticles, the dielectric loss ability of the obtained nanocomposite absorber has been greatly improved. Considering the $Co_{0.2}Fe_{2.8}O_4$ magnetic nanoparticles caused magnetic loss, the MWCNTs/Ag/ $Co_{0.2}Fe_{2.8}O_4$ nanocomposite absorber has the better EM wave attenuation performance. Additionally, it can also be an evidence for the importance of the specially designed nanostructure in determining the EM wave absorption characteristic of the nanocomposite absorber.

In this MWCNTs based nanocomposite absorber, Ag nanoparticles and $Co_{0.2}Fe_{2.8}O_4$ nanoparticles are introduced to enhance the EM wave absorbency of MWCNTs. The introduction of Ag nanoparticles to the nanocomposite may effectively enhance the interfacial polarization between the Ag nanoparticles and carbon as well as Ag nanoparticles and $Co_{0.2}Fe_{2.8}O_4$ nanoparticles. The enhanced interfacial polarization is due to the formation of a heterogeneous system and more interface, as well as the stronger coupling at the gaps between the adjacent Ag nanoparticles. [52] As a result, the enhanced interfacial polarization can contribute to the EM wave absorption. [53] Moreover, the introduction of $Co_{0.2}Fe_{2.8}O_4$ nanoparticles is also necessary. It is well known that $Co_{0.2}Fe_{2.8}O_4$ nanoparticles are magnetic loss absorbents. At the same time, there are dipoles present in $Co_{0.2}Fe_{2.8}O_4$ nanoparticles especially when their sizes are at the nanoscale. The number of surface atoms with unsaturated bonds greatly increase as the size decrease, causing an increase in dipoles. [54] As schematically shown in Figure 7b, the interactions among MWCNTs, $Co_{0.2}Fe_{2.8}O_4$ and Ag would cause multiple interfacial polarization, resulting associated relaxation loss under an EM field. And the assembled movements of collective interfacial dipoles at the interfaces could zoom up the response to incident EM wave and thus improve the EM wave absorption performance. Consequently, the dipole polarizations can contribute to the dielectric loss. The Debye dipolar relaxation for all the samples was further investigated in the supporting information (SI-5, Figure S8) to explain the dielectric loss ability. The plot of ε' *vs.* ε'' would be a single semicircle, generally denoted as the Cole-Cole semicircle. Each semicircle corresponds to one Debyerelaxation process. [55] For MWCNTs/Ag/$Co_{0.2}Fe_{2.8}O_4$ shown in Figure S8c, it can be seenclearly that three segment semicircles were obtained,

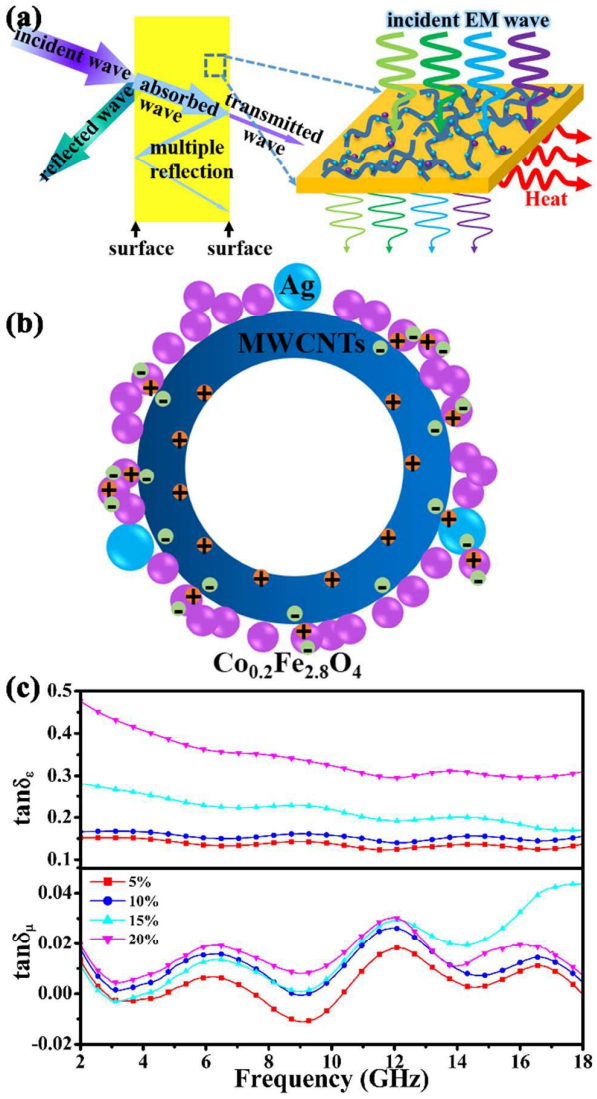

Fig. 7. (a) The scheme of the EM wave attenuation process in the absorber; (b) Schematic illustration of multiple interfacial dipoles within MWCNTs/Ag/$Co_{0.2}Fe_{2.8}O_4$; (c) The loss tangent of MWCNTs/Ag/$Co_{0.2}Fe_{2.8}O_4$ with absorber content of 5%, 10%, 15%, and 20%. The dielectric loss tangent and magnetic loss tangent have the same curve label.

suggesting that there are multi-dielectric relaxation processes in the nanocomposite absorber. To clearly verify the origin of the relaxation processes, the Debye relaxation characteristic of MWCNTs and MWCNTs/Ag were also sketched in Figure S8a and S8b. MWCNTs and MWCNTs/Ag all present a clear segment of two semicircles. However, the widths of the semicircles of MWCNTs/Ag are larger than that of MWCNTs. It demonstrates that Ag nanoparticles can improve the intensity of the Debye dipolar relaxation process. For MWCNTs/Ag/$Co_{0.2}Fe_{2.8}O_4$, one more semicircle appeared, indicating the presence of $Co_{0.2}Fe_{2.8}O_4$ can increase the number of the relaxation processes of the nanocomposite absorber. Accordingly, the special designed nanostructure has influence on Debye dipolar relaxation which could also account

for the special dielectric loss ability for MWCNTs/Ag/$Co_{0.2}Fe_{2.8}O_4$.

Ultimately, as mentioned above, MWCNTs/Ag/$Co_{0.2}Fe_{2.8}O_4$ exhibits tunable EM wave absorption characteristic with the strong EM absorbency, the thin matching thickness and the wide EM wave absorption band width. The excellent EM wave attenuation ability of this nanocomposite is due to three main factors: Firstly, the introduction of $Co_{0.2}Fe_{2.8}O_4$ nanoparticles with a relatively low conductivity can effectively reduce the reflection of EM wave on the surface of the absorber and paraffin wax composite. Thus EM wave can propagate into the absorber to be attenuated. Secondly, the Ag nanoparticles can improve the intensity of the Debye dipolar relaxation process. Thirdly, the introduction of Ag nanoparticles and $Co_{0.2}Fe_{2.8}O_4$ nanoparticles to the nanocomposite can be an effective way to enhance the interfacial polarization for the formation of more interfaces (Ag/C, Ag/ $Co_{0.2}Fe_{2.8}O_4$, and $Co_{0.2}Fe_{2.8}O_4$/C), as well as the stronger coupling at the gaps between the adjacent Ag nanoparticles. Therefore, the incident EM wave can be attenuated by the dielectric loss for the strong interfacial polarization and Debye dipolar relaxation. Lastly, though the dielectric loss contributes the most to the EM absorbency, the magnetic component ($Co_{0.2}Fe_{2.8}O_4$ nanoparticles) caused magnetic loss can also be an indispensable part of the EM wave attenuation ability. The combination of the dielectric loss and the magnetic loss can result in a fine EM wave absorption. Consequently, the multiple factors lead to the remarkable EM wave absorption properties of the MWCNTs/Ag/$Co_{0.2}Fe_{2.8}O_4$ nanocomposite.

Conclusions

MWCNTs/Ag/$Co_{0.2}Fe_{2.8}O_4$ was successfully synthesized, and the structure, morphology and composition have been investigated in detail. It is evident that MWCNTs/Ag/$Co_{0.2}Fe_{2.8}O_4$ has an excellent EM wave attenuation ability with tunable absorption characteristic. At the absorber loading of 20%, MWCNTs/Ag/$Co_{0.2}Fe_{2.8}O_4$ demonstrated the highest absorbency value of -52.4 dB at 10.2 GHz with the absorber thickness of 1.8 mm. Moreover, with the absorber thickness from 1.1 to 3.7 mm, the nanocomposite absorber shows a strong absorbency for EM wave in the C band, the X band and the K_u band with the minimum RL values below -20 dB (99% attenuation). Thus, the nanocomposite has great potential to be a highly efficient and lightweight EM wave absorber in 4-18 GHz. The excellent EM wave attenuation ability results from the strong interfacial polarization caused dielectric loss and the combination of the dielectric loss and the magnetic loss for the cooperation of Ag and $Co_{0.2}Fe_{2.8}O_4$ nanoparticles with MWCNTs. Our results demonstrate that MWCNTs/Ag/$Co_{0.2}Fe_{2.8}O_4$ would be a promising and attractive material for application in EM wave absorption field.

Acknowledgements

This work was financially supported by the Science and Technology Department of Jilin Province Foundation (20130204026GX). Also the authors express their great thanks for the kindly help of M.S. Yue Zhao from the State Key Laboratory of Inorganic Synthesis and Preparative Chemistry and Prof. Lifeng Wang from Alan G. MacDiarmid Institute in structural characterization.

References

1. Y. F. Zhu, Q. Q. Ni and Y. Q. Fu, *RSC Adv*, 2015, **5**, 3748-3756.
2. B. A. Zhao, G. Shao, B. B. Fan, W. Y. Zhao, Y. Q. Chen and R. Zhang, *RSC Adv*, 2015, **5**, 9806-9814.
3. B. Zhao, G. Shao, B. B. Fan, W. Y. Zhao, Y. J. Xie and R. Zhang, *RSC Adv*, 2014, **4**, 61219-61225.
4. L. Yuan, L. X. Xuan, L. Rong and L. Ying, *RSC Adv*, 2015, **5**, 18660-18665.
5. G. Tong, W. Wu, Q. Hua, Y. Miao, J. Guan and H. Qian, *J Alloy Compd*, 2011, **509**, 451-456.
6. Z. H. Yang, Z. W. Li, L. H. Yu, Y. H. Yang and Z. C. Xu, *J Mater Chem C*, 2014, **2**, 7583-7588.
7. Y. L. Ren, C. L. Zhu, L. H. Qi, H. Gao and Y. J. Chen, *RSC Adv*, 2014, **4**, 21510-21516.
8. X. B. Li, S. W. Yang, J. Sun, P. He, X. P. Pu and G. Q. Ding, *Synthetic Met*, 2014, **194**, 52-58.
9. D. P. Sun, Q. Zou, Y. P. Wang, Y. J. Wang, W. Jiang and F. S. Li, *Nanoscale*, 2014, **6**, 6557-6562.
10. Z. Zhonglun, J. Zhijiang, D. Yuping, G. Shuchao and G. Jingbo, *J Mater Sci: Mater Electron*, 2013, **24**, 968-973.
11. X. H. Li, J. Feng, H. Zhu, C. H. Qu, J. T. Bai and X. L. Zheng, *RSC Adv*, 2014, **4**, 33619-33625.
12. M. Verma, A. P. Singh, P. Sambyal, B. P. Singh, S. K. Dhawan and V. Choudhary, *Phys Chem Chem Phys*, 2015, **17**, 1610-1618.
13. M. Zeng, J. Liu, R. H. Yu and M. G. Zhu, *Ieee T Magn*, 2014, **50**.
14. H. Wu, L. Wang, Y. Wang, S. Guo and Z. Shen, *Materials Science and Engineering: B*, 2012, **177**, 476-482.
15. J. C. Wang, H. Zhou, J. D. Zhuang and Q. Liu, *Phys Chem Chem Phys*, 2015, **17**, 3802-3812.
16. B. Zhao, G. Shao, B. B. Fan, W. Y. Zhao and R. Zhang, *Phys Chem Chem Phys*, 2015, **17**, 2531-2539.
17. M. S. Cao, J. Yang, W. L. Song, D. Q. Zhang, B. Wen, H. B. Jin, Z. L. Hou and J. Yuan, *Acs Appl Mater Interfaces*, 2012, **4**, 6948-6955.
18. S. Varshney, A. Ohlan, V. K. Jain, V. P. Dutta and S. K. Dhawan, *Ind Eng Chem Res*, 2014, **53**, 14282-14290.
19. Z. F. He, Y. Fang, X. J. Wang and H. Pang, *Synthetic Met*, 2011, **161**, 420-425.
20. B. Wen, M. S. Cao, M. M. Lu, W. Q. Cao, H. L. Shi, J. Liu, X. X. Wang, H. B. Jin, X. Y. Fang, W. Z. Wang and J. Yuan, *Adv Mater*, 2014, **26**, 3484-3489.
21. K. Hayashida and Y. Matsuoka, *Carbon*, 2015, **85**, 363-371.
22. D. Micheli, A. Vricella, R. Pastore and M. Marchetti, *Carbon*, 2014, **77**, 756-774.
23. A. P. Singh, M. Mishra, D. P. Hashim, T. N. Narayanan, M. G. Hahm, P. Kumar, J. Dwfuedi, G. Kedawat, A. Gupta, B. P. Singh, A. Chandra, R. Vajtai, S. K. Dhawan, P. M. Ajayan and B. K. Gupta, *Carbon*, 2015, **85**, 79-88.
24. W. L. Song, M. S. Cao, L. Z. Fan, M. M. Lu, Y. Li, C. Y. Wang and H. F. Ju, *Carbon*, 2014, **77**, 130-142.
25. J. J. Jiang, D. Li, S. J. Li, Z. H. Wang, Y. Wang, J. He, W. Liu and Z. D. Zhang, *RSC Adv*, 2015, **5**, 14584-14591.
26. B. A. Zhao, G. Shao, B. B. Fan, W. Y. Zhao and R. Zhang, *Phys Chem Chem Phys*, 2015, **17**, 6044-6052.
27. J. Fang, Z. Chen, W. Wei, Y. Li, T. Liu, Z. Liu, X. Yue and Z. Jiang, *RSC Adv*, 2015, **5**, 50024-50032.

28. Y. Qing, W. Zhou, F. Luo and D. Zhu, *Carbon*, 2010, **48**, 4074-4080.
29. G. Tong, F. Liu, W. Wu, F. Du and J. Guan, *J Mater Chem A*, 2014, **2**, 7373.
30. G. Tong, Y. Liu, F. Liu and J. Guan, *Surf. Coat. Technol.*, 2015, **283**, 286-297.
31. J. Qiu and T. T. Qiu, *Carbon*, 2015, **81**, 20-28.
32. L. Kong, X. W. Yin, M. K. Han, L. T. Zhang and L. F. Cheng, *Ceram Int*, 2015, **41**, 4906-4915.
33. Y. Liu, X. X. Liu and X. J. Wang, *Chinese Physics B*, 2014, **23**.
34. Z. Zhang, F. Zhang, X. Jiang, Y. Liu, Z. Guo and J. Leng, *Fibers Polym*, 2014, **15**, 2290-2296.
35. H. L. Zhu, Y. J. Bai, R. Liu, N. Lun, Y. X. Qi, F. D. Han and J. Q. Bi, *J Mater Chem*, 2011, **21**, 13581-13587.
36. J. Wei, S. Zhang, X. Y. Liu, J. Qian, J. S. Hua, X. X. Li and Q. X. Zhuang, *J Mater Chem A*, 2015, **3**, 8205-8214.
37. F. S. Wen, F. Zhang and Z. Y. Liu, *J Phys Chem C*, 2011, **115**, 14025-14030.
38. W. Wei, X. Yue, Y. Zhou, Z. Chen, J. Fang, C. Gao and Z. Jiang, *Phys Chem Chem Phys*, 2013, **15**, 21043-21050.
39. K.-Y. Pan, Y.-F. Liang, Y.-C. Pu, Y.-J. Hsu, J.-W. Yeh and H. C. Shih, *Appl Surf Sci*, 2014, **311**, 399-404.
40. K. R. Reddy, B. C. Sin, K. S. Ryu, J.-C. Kim, H. Chung and Y. Lee, *Synthetic Met*, 2009, **159**, 595-603.
41. Y. C. Du, W. W. Liu, R. Qiang, Y. Wang, X. J. Han, J. Ma and P. Xu, *Acs Appl Mater Interfaces*, 2014, **6**, 12997-13006.
42. W. Wei, X. Yue, Y. Zhou, Y. Wang, Z. Chen, M. Zhu, J. Fang and Z. Jiang, *RSC Adv*, 2014, **4**, 11159-11167.
43. F. Qin and C. Brosseau, *J Appl Phys*, 2012, **111**, 061301.
44. L. Yuan, L. Xiangxuan, L. Rong, W. Wu and W. Xuanjun, *RSC Adv*, 2015, **5**, 8713-8720.
45. G. Liu, L. Y. Wang, G. M. Chen, S. C. Hua, C. Q. Ge, H. Zhang and R. B. Wu, *J Alloy Compd*, 2012, **514**, 183-188.
46. J. Xiang, J. L. Li, X. H. Zhang, Q. Ye, J. H. Xu and X. Q. Shen, *J Mater Chem A*, 2014, **2**, 16905-16914.
47. H. L. Lv, G. B. Ji, H. Q. Zhang and Y. W. Du, *RSC Adv*, 2015, **5**, 76836-76843.
48. G. J. H. Melvin, Q. Q. Ni and T. Natsuki, *J Alloy Compd*, 2014, **615**, 84-90.
49. X. Meng, Y. Wan, Q. Li, J. Wang and H. Luo, *Appl Surf Sci*, 2011, **257** 10808-10814.
50. C. Feng, X. G. Liu, Y. P. Sun, C. G. Jin and Y. H. Lv, *RSC Adv*, 2014, **4**, 22710-22715.
51. B. Zhao, G. Shao, B. B. Fan, W. Y. Zhao, Y. J. Xie and R. Zhang, *Phys Chem Chem Phys*, 2015, **17**, 8802-8810.
52. T. Long, L. Hu, H. X. Dai and Y. X. Tang, *Appl Phys A-mater*, 2014, **116**, 25-32.
53. J. L. Guo, X. L. Wang, P. L. Miao, X. P. Liao, W. H. Zhang and B. Shi, *J Mater Chem*, 2012, **22**, 11933-11942.
54. G. Z. Liu, W. Jiang, Y. P. Wang, S. T. Thong, D. P. Sun, J. Liu and F. S. Li, *Ceram Int*, 2015, **41**, 4982-4988.
55. H. Yu, T. Wang, B. Wen, M. Lu, Z. Xu, C. Zhu, Y. Chen, X. Xue, C. Sun and M. Cao, *J Mater Chem*, 2012, **22**, 21679-21685.

MWCNTs and nanoparticles composite as a high efficient and lightweight electromagnetic wave absorber in 4-18 GHz

Jiyong Fang, Yan Wang, Wei Wei, Zheng Chen, Yunxi Li, Zhi Liu, Xigui Yue* and Zhenhua Jiang

Corresponding author: Xigui Yue

E-mail addresses: yuexigui@jlu.edu.cn

Tel: +86 431 85168868

The key laboratory for high performance polymer of the Ministry Education of China, College of Chemistry, Jilin University, 2699 Qianjin street, Changchun 130012, People's Republic of China

Graphic abstract:

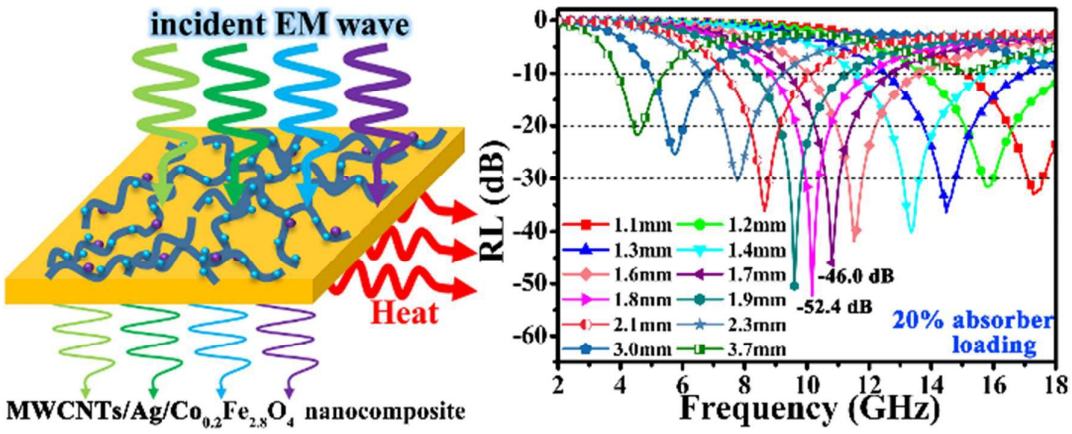

The nanocomposite absorber has an excellent EM wave attenuation ability with the wide absorption band (4-18 GHz), the strong absorption (minimum RL value of -52.4 dB at 10.2 GHz) and the thin absorber thickness (RL value of -52.4 dB at 1.8 mm, and the strong absorption in 4-18 GHz with thickness of 1.1-3.7 mm). It is believed that such a nanocomposite could serve as an attractive candidate for EM wave attenuation application in the future.